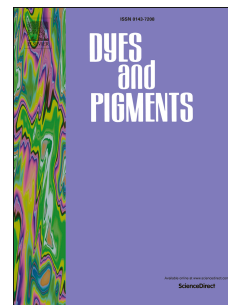


Accepted Manuscript

Synthesis and structural characterization of 2,3,7,8,12,13,17,18-octakis(propyl), N, N, N', N'-tetramethylaminoporphyrazines and 2,3,9,10,16,17,23,24-octa substituted phthalocyanine and the kinetic studies of their Co(II) and Cu(II) metalated complexes

David Isabirye , Fanyana Mtunzi , Temitayo Aiyelabola



PII: S0143-7208(14)00193-4

DOI: [10.1016/j.dyepig.2014.05.013](https://doi.org/10.1016/j.dyepig.2014.05.013)

Reference: DYPI 4385

To appear in: *Dyes and Pigments*

Received Date: 11 March 2014

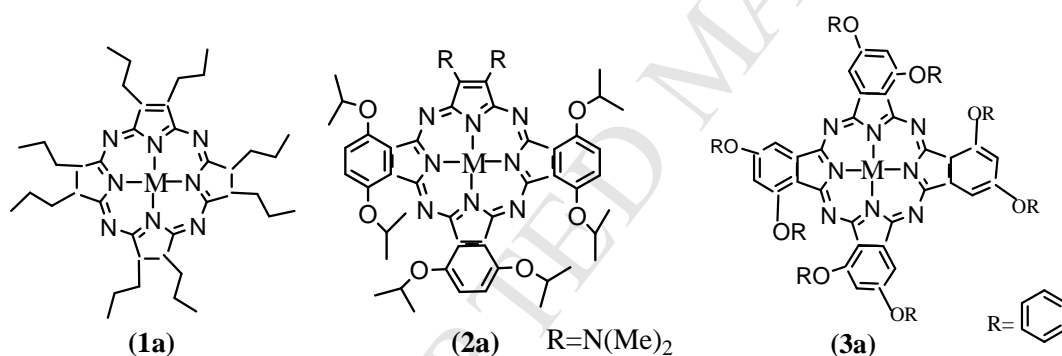
Revised Date: 29 April 2014

Accepted Date: 9 May 2014

Please cite this article as: Isabirye D, Mtunzi F, Aiyelabola T, Synthesis and structural characterization of 2,3,7,8,12,13,17,18-octakis(propyl), N, N, N', N'-tetramethylaminoporphyrazines and 2,3,9,10,16,17,23,24-octa substituted phthalocyanine and the kinetic studies of their Co(II) and Cu(II) metalated complexes, *Dyes and Pigments* (2014), doi: 10.1016/j.dyepig.2014.05.013.

This is a PDF file of an unedited manuscript that has been accepted for publication. As a service to our customers we are providing this early version of the manuscript. The manuscript will undergo copyediting, typesetting, and review of the resulting proof before it is published in its final form. Please note that during the production process errors may be discovered which could affect the content, and all legal disclaimers that apply to the journal pertain.

- Three tetrapyrrole macrocyclic compounds 2,3,7,8,12,13,17,18-octakis(propyl)porphyrazine **1a**, N, N, N', N'-tetramethylamino porphyrazine hybrid **2a** and 2,3,9,10,16,17,23,24-octa substituted phthalocyanine **3a** were synthesized and characterized using elemental analysis, FTIR, ^1H , ^{13}C NMR and UV-Vis spectroscopic techniques.
- Kinetics of their metalation with Co(II) and Cu(II) and redox reaction of the complexes was studied and reported for the first time.
- It was suggested that for the incorporation of the metal ion, deformation of the ring was essential for effective coordination; and this was a function of the metal ion size and peripheral functionalities of the ligands.
- The spectroelectrochemical studies for the redox reactions indicated metal based oxidation for the reductants and ring based reduction for the oxidants. An outer sphere electron tunneling mechanism was proposed for the redox reaction.
- It further showed that the redox activity of the metal ions was dependent on the availability of their low energy d-orbitals. It was therefore inferred that the nature of the metal ion and the peripheral substituents of these tetrapyrrole macrocyclic compounds and their complexes had a significant effect on their reactivity.



Synthesis and structural characterization of 2,3,7,8,12,13,17,18-octakis(propyl), N, N, N', N'-tetramethylaminoporphyrazines and 2,3,9,10,16,17,23,24-octa substituted phthalocyanine and the kinetic studies of their Co(II) and Cu(II) metalated complexes

David Isabirye^{a*}, Fanyana Mtunzi^b and Temitayo Aiyelabola^a

^aDepartment of Chemistry, North-West University, Private Bag X 2046. Mmabatho 2735, South Africa.

^bDepartment of Chemistry, Vaal University of Technology, Private Bag X021, Vanderbijlpark 1900, South Africa.

Abstract

Three tetrapyrrole macrocyclic compounds 2,3,7,8,12,13,17,18-octakis(propyl)porphyrazine, N, N, N', N'-tetramethylamino porphyrazine hybrid and 2,3,9,10,16,17,23,24-octa substituted phthalocyanine were synthesized and characterized using elemental analysis, FTIR, ¹H, ¹³C NMR and UV-vis spectroscopic techniques. Kinetics of their metalation with Cu(II) and Co(II) and redox reaction of the complexes was studied and are reported here for the first time. It is suggested that deformation of the ring, which is a function of their peripheral functionalities, is essential for effective coordination of the ligands. The kinetic studies indicated metal based oxidation and ring based reduction for the reductants and oxidant respectively. The redox activity of the metal ions is dependent on the availability of their low energy level *d*-orbitals for charge transfer. It was therefore inferred that the nature of the metal ion and the peripheral substituents of these ligands and their complexes had significant effect on their reactivity.

Keywords: Porphyrazine hybrid, porphyrazine, phthalocyanine, metalation kinetics, redox reaction

*Corresponding author. Tel: +27 18 3892308; Fax,+27 18 3892052; E.mail address: David.Isabirye@nwu.ac.za

1.0 Introduction

The synthesis, properties and application of porphyrazines (Pzs) and metaloporphyrazines (MPzs) have received increasing attention in recent years [1]. This is due to their varied potential in technological applications such as sensors and photocatalyst for energy conversion processes [2, 3]. They have also found usage as photosensitizers in photodynamic therapy and as biomedical imaging agents [1]. This has been encouraged partly because of their effective absorbance in the blue region of the visible spectrum, low cost of synthesis and lack of toxicity [4, 5]. Tetrapyrrole macrocycles porphyrins (Ps), porphyrazines (Pzs) and phthalocyanines (Pcs) are isoelectronic. They can thus be viewed as variants of each other; hence their reactivity may therefore be compared. Unlike the other two macrocycles however porphyrazines have been less studied [1, 6-8].

Peripheral functionalization of Pzs has resulted in the significant modulation of their physical and chemical properties [1, 6, 8]. This functionalization can be either symmetrical or unsymmetrical. Unsymmetrical peripheral functionalization includes the porphyrazine hybrid which combines the electronic character and extended π electron system of porphyrazines and phthalocyanines [6, 9-11]. Another way in modifying the properties of these Pzs is the use of various transition metal ions incorporated in their inner core [1]. As a consequence, an investigation of the relationship involving their chemical structure, the kinetics of formation and redox reactions of MPzs is important. This is because it may provide useful understanding in designing synthetic pathways to new compounds and also provide information on the mechanism of the reactions. Furthermore, such studies would also yield information essential for understanding their implementation in many technological areas such as electrophotography, photovoltaic cells, fuel cells and electrochromic displays [8].

In contrast to the metaloporphyrins (MPs) the mechanism of formation for MPcs and MPzs is yet to be exhaustively studied. Focus has been on their synthesis, characterization and electrochemistry [6, 8]. In this regard the aim of the present study was to synthesize symmetrical porphyrazine **1a**, porphyrazine hybrid **2a** and phthalocyanine **3a** derivatives and study the kinetics of incorporation of copper(II) and cobalt(II) ions into the central cavity of the synthesized ligands to give **1b**, **2b**, **3b**, **1c**, **2c** and **3c** respectively. In addition, study the redox reaction of their complexes, and then propose the mechanism for both reactions.

2.0 Material and methods

2.1 General

All solvents used were purified according to standard literature techniques and the reactions were done under nitrogen atmosphere. Flash column chromatography was carried out on Merck Kieselgel 60 (230-400 mesh) under

nitrogen pressure. Thinlayer chromatography was performed using Merck 60 F₂₅₄ silica gel sheets. NMR spectra were recorded on a Varian Gemini 300 MHz spectrometer in CDCl₃. Electronic spectra were measured on a Varian Cary 50 ultraviolet-visible spectrophotometer, using a matched pair of 1 cm path length quartz cuvettes, measurements were made from 300 nm to 800 nm. Infra-red spectra was recorded on a Nicolet 410 impact fourier transform infrared spectrophotometer using nujol or potassium bromide cells, in the range 4000 cm⁻¹ and 500 cm⁻¹. Compounds **4-6** and **8-10** were prepared according to published procedures, [9, 12].

2.2 Synthesis of the compounds

2.2.1 Synthesis of 2,3,7,8,12,13,17,18-octakis(propyl)porphyrizinato magnesium(II) **1d**.

Compound **1d** was prepared according to established method (**Figure 1**) [6]. Butanol (20 ml), magnesium (0.077 g, 3.17 mmol) and iodine crystals were refluxed for 24 hours after which 2,3-dipropylmaleonitrile, **7** (0.300 g, 0.831 mmol) was added to the suspension of magnesium butoxide and the reaction mixture refluxed for the 24 hours away from direct light. The brownish purple solution obtained was evaporated and the residue was re-dissolved in ethyl acetate. It was then purified using flash column chromatography with ethyl acetate: dichloromethane (1:10) solvent system. Yield = 92 mg, 0.136 mol; %Yield = 4.3; R_f = 0.61, ethyl acetate: dichloromethane (1:10). IR ν (cm⁻¹): 3395 (C-H) aromatic, 2928-2851 (CH₂, CH₃), 1643 (C=C), 1379 (C-H), 470 (N-Mg). Uv-vis λ_{\max} (nm): 345, 550, 600. ¹H NMR (300 MHz, CDCl₃) δ 1.35 (t, 24H, J=7.5Hz), 2.52 (hp, 16H, J=7.4Hz), 4.06(t, 16H, J=7.5Hz); ¹³C NMR (300 MHz, CDCl₃) δ 15.20, 26.22, 28.84, 30.08, 30.59, 122.78, 123.17, 123.50, 123.83, 134.81, 135.17, 135.50, 135.82, 143.92, 149.47, 149.83, 150.19, 158.82. Anal Calcd: C, 68.05; H, 7.31; N, 19.30. Found: C, 68.93; H, 7.28; N, 20.00.

2.2.2 Synthesis of 2,3,7,8,12,13,17,18-octakis(propyl)porphyrazine **1a**

Removal of magnesium from **1d** (0.58 g) was accomplished by heating it at reflux in a CHCl₃/TFA (20:1) solution (200 ml), which was made basic by the addition of NaOH. The organic layer was separated, washed once with 10% aqueous NaOH (50 ml), anhydrous Na₂SO₄ and filtered. **1a** was adsorbed onto a silica gel, column chromatographed and eluted with CH₂Cl₂/Hexane (1:1). Slow evaporation of the solvent gave a microcrystalline solid, which was recrystallized by slow diffusion of benzene into a CHCl₃ solution of the free base Yield = 0.48g, %Yield = 0.827, R_f = 0.413 (Hexane: ethyl acetate, 10:1). IR ν (cm⁻¹): 3021 (N-H), 2928-2851 (CH₂, CH₃), 1209 (C=C), 723 (C-H). Uv-vis λ_{\max} (nm): 339, 558, 626. ¹H NMR (CDCl₃) δ = -2.11 (s, 2H, NH), 1.86 (t, 24H, J = 7.7 Hz, CH₃), 3.98 (q, 16H, J = 7.7 Hz, CH₂CH₂CH₃). Anal Calcd: C, 71.74; H, 7.97; N, 20.29. Found: C, 71.68; H, 8.01; N, 20.28.

2.2.3 Synthesis of N, N, N', N'-tetramethylamino porphyrazine hybrid **2a**

The synthesis of **2a** was achieved by a modification of previously reported method by Forsyth et al. (**Figure 2**) [9]. Butanol (30 ml) and magnesium (0.210 g, 8.64 mmol) were refluxed for 24 hours. This was followed by addition of bis(dimethylamino) maleonitrile, **11** (0.270 g, 1.642 mmol) in butanol (5 ml) and 4,7-(isopropoxy)-1,3-iminoisoindoline, **12** (1.230 g, 4.701 mmol) in butanol (5 ml) in suspension of magnesium butoxide. The reaction mixture was refluxed for the 24 hours away from direct light. After which the brownish purple solution obtained was evaporated under reduced pressure and the residue was re-dissolved in dichloromethane (60 ml) followed by addition of trifluoroacetic acid (20 ml). The resultant product was vigorously stirred for 2 hours in an ice-bath. After 2 hours the reaction mixture was poured into ice cold concentrated ammonium hydroxide (50 ml) and stirred for 30 minutes. After this, the aqueous and organic layers were separated. The aqueous layer was further extracted with dichloromethane (3 x 150 ml) and the two organic layers were mixed and dried with anhydrous sodium sulphate. The sodium sulphate was filtered off and the solvent evaporated under reduced pressure. The sample mixture was purified by flash column chromatography packed with silica gel using ethyl acetate: dichloromethane: toluene (1:8:6) solvent system as eluent. Three components were separated as pure fractions. The bulk sample was re-separated using a mixture of ethyl acetate: dichloromethane: toluene (0.5: 1: 4) as eluent on flash silica. The major product **2a** was separated as pure. Yield = 97 mg, 0.108 mmol, % Yield = 6.6. IR ν (cm⁻¹): 3508 (N-H), 1593 (C=C), 1265 (C-H), 1040 (C-H) Uv-vis λ_{\max} (nm): 325, 556, 742. ¹H NMR (300MHz, CDCl₃) δ : (s, 6H), 4.95 (m, 1H), 5.10 (m, 1H), 5.17 (m, 1H), 7.37 (d, 2H, J=9Hz), 7.46 (d, 2H, J=8.7Hz); ¹³C (300MHz, CDCl₃) δ 22.71, 22.78, 30.97, 44.57, 70.77, 75.24, 75.53, 114.50, 122.58, 124.26, 125.06, 128.54, 128.77, 130.84, 131.02, 135.05, 140.73, 140.80, 148.63, 150.48, 150.97. Anal Calcd: C, 64.49; H, 7.29 N, 6.47. Found: C, 65.63; H, 7.88; N, 6.73.

2.2.4 Synthesis of 2,3,9,10,16,17,23,24-octa substituted phthalocyanine **3a**

1,2-Diisocyano-4-phenoxy benzene, **13** (0.300 g, 1.36 x 10⁻³ mol) was refluxed in 1-pentanol, **14** (14 ml). The resulting product **15** was refluxed further in the presence of 1 mol 1,8-Diazabicyclo[5.4.0]-undec-7-ene (0.21 g, 1.36 x 10⁻³ mol) for 16 hours (**Figure 3**). Methanol (20 ml) was there after added and the precipitate **3a** filtered, soxhlet extracted with methanol and acetone and dried at 60° C. Yield = 0.294g, % Yield = 43 R_f=0.23 (ethyl acetate: hexane, 3:8). IR ν (cm⁻¹): 3620 (N-H), 2848 (C-H) aromatic, 1685 (C=C), 1163 (C-H), 743 (C-H). Uv-vis λ_{\max} (nm): 337, 606, 640, 661, 702. ¹H NMR (300MHz, CDCl₃) δ -2.01 (s, 2H, NH), 3.66 (m, 4H, CH), 6.99 (m, 4H, ArH), 7.23 (m, 4H, ArH), 7.50 (m, 4H, ArH) 8.04 (m, 4H, ArH), 8.99 (m, 4H, ArH), 9.23 (m, 4H, ArH), ¹³C NMR (300MHz,

CDCl_3) δ 71.01, 76.57, 76.99, 77.41, 117.45, 119.69, 119.92, 126.95, 127.48, 127.63, 128.53, 128.85, 128.94, 134.43, 135.20. Anal Calcd: C, 76.21; H, 4.19; N, 9.03. Found: C, 76.21; H, 4.18; N, 9.11.

2.2.5 Synthesis of the complexes

The synthesis of the complexes of **1a**, **2a** and **3b** was carried out by an adaptation of established method as described by Forsyth et al. [9]. 0.01M solution of appropriate metal salts of cobalt(II) acetate and copper(II) acetate was dissolved in ethanol and added to 0.015 M solution of **1a**, **2a** and **3b** in dichloromethane with stirring until a uniform solution was achieved. The mixture was heated for 2 h under nitrogen controlled environment. Immediate precipitate was obtained for majority of the complexes. The solvents were removed using a rotary evaporator and the products obtained filtered, washed and dried in vacuo at 60 °C.

2.3 Kinetics studies

2.3.1 Metalation

The reactions were monitored spectrophotometrically by a Varian Cary 50 ultraviolet-visible spectrophotometer with a thermostated cell compartment maintained at 25 °C \pm 0.1. Metalation of the ligands was carried out in 1 cm cells by mixing solutions of the ligands and that of the corresponding metal ion solution, copper acetate or cobalt acetate, pre-equilibrated at the reaction temperature. The Uv-vis absorption spectrum was scanned from 300 to 800 nm and readings were taken at constant wavelength. The absorption spectra changed as a function of time with distinct isobestic points until completion of the reaction. The kinetics was run under pseudo-first order conditions with the metal ion concentration at a large excess over that of the corresponding free base ligand.

2.3.2 Redox

Solutions of **1c**, **2c** and **3c** in dichloromethane were allowed to equilibrate at 25 °C under nitrogen. Solutions of **1b** in glacial acetic acid under nitrogen was also prepared and allowed to equilibrate at 25 °C. The solutions were mixed and quickly transferred to a 1 cm quartz cell in a thermostated compartment of the Cary 50 spectrophotometer. The Uv-vis absorption spectrum from 300 to 800 nm was scanned and readings were taken. The absorption spectra changed as a function of time with distinct isobestic points until completion of the reaction.

3.0 Results and Discussion

3.1 Characterization of compounds

The structure of the compounds was confirmed using elemental analysis, FTIR, ^1H , ^{13}C NMR and UV-vis spectroscopic techniques. The elemental analysis results obtained are in close agreement with the calculated values. Spectral assignment of the compounds was achieved by the comparison of the spectra of the compounds with those of their starting material and that of similar compounds.

3.1.1 2,3,7,8,12,13,17,18-octakis(propyl)porphyrzine **1a**

The ^1H NMR spectrum of **1a** displayed a broad peak at -2.11 ppm diagnostic of the N-H protons in its inner core. Similar peaks have been reported to be indicative of the shielding of the pyrrolic nitrogen atoms of porphyrzines [13, 14]. Consequently confirming the formation of the macrocycle and hence the demetalation of **1d**. Evidence of the cyclotetramerization of the dinitrile was given by the absence of the $\text{C}\equiv\text{N}$ band in this spectrum. This was however observed at 3.00 ppm in the spectrum of **7**, dipropylmalenitrile, one of the starting material [15]. A triplet observed at 1.86 ppm was assigned to the methyl protons of the propyl substituents. The triplet at 3.98 ppm corresponds to protons attached to carbon of the propyl substituent linked to the pyrrole rings $\text{CH}_2\text{CH}_2\text{CH}_3$. The infrared spectrum of **1a** on the other hand showed a weak band at 3021 cm^{-1} indicative of the two protonated nitrogen atoms in the inner core of the porphyrzine ring, suggesting **1a** was metal free. This was further corroborated by the absence of the N-Mg stretching frequency in the spectrum of **1a** observed at 470 cm^{-1} for **1d** [16]. The most revealing data for a tetrapyrrole macrocyclic system is given by its UV-vis spectra in solution [1]. Metal containing porphyrzines have D_{4h} symmetry consequently the Q band appears as one peak in the visible spectrum. The symmetry of the metal-free macrocycle is however reduced to D_{2h} and the Q band splits into two distinct bands. The electronic spectrum of **1d** exhibited a Q-band at $\lambda_{\text{max}} = 600\text{ nm}$, which was however split into Q_x [$\lambda_{\text{max}} = 558\text{ nm}$] and Q_y [$\lambda_{\text{max}} = 626\text{ nm}$] in **1a** spectrum. This indicated that the Q-band shifted from D_{4h} in **1d** to D_{2h} symmetry in **1a** [13, 14].

3.1.2 N, N, N', N'-tetramethylamino porphyrzine hybrid **2a**

The ^1H NMR of **2a** is in close agreement with that obtained for similar compounds in literature [9]. The spectrum exhibited a singlet at 1.23 ppm, which was assigned to the protonated pyrrolic nitrogen in the core of the molecule, typical of tetrapyrrole macrocycles with electron donating substituents [17]. This is suggestive of the demetalation of **2a**. The signal at 1.52 ppm a doublet of doublets and another doublet at 1.70 ppm were ascribed to protons of the methyl substituents attached to the carbons linked to the phenoxy group. This corresponds to the *trans* and *cis*-

methyl substituents respectively. A singlet at 3.7 ppm was due to the protons attached to nitrogen of the substituents [N(Me)₂]. The signal at 5.15 ppm, a multiplet was attributed to the protons of the carbon attached directly to the phenoxy oxygen. A singlet at 7.37 ppm was ascribed to the proton of the methine carbon on the phenoxy ring [1, 9, 15]. The infrared spectrum of **2a** showed characteristic N-H stretching frequency observed at 3508 cm⁻¹. This supports the formation of the macrocycle. Isoindole and C-H bending were observed at 1040 and 1265 cm⁻¹. Pyrrole breathing was observed at 1137-1198 cm⁻¹. Aromatic C=C and C-H peaks were observed at 1593 cm⁻¹ and 3329 cm⁻¹ respectively [15, 16, 18, 19]. Formation of the macrocycle was further confirmed by its electronic spectrum which showed an intense B (soret) band at $\lambda_{\text{max}} = 325$ nm and a Q-band that was split into Q_x [$\lambda_{\text{max}} = 556$ nm] and Q_y [$\lambda_{\text{max}} = 742$ nm]. This was assigned to $\pi \rightarrow \pi^*$ transitions of the macrocycle. The shoulder at $\lambda_{\text{max}} = 650$ nm was assigned to $n \rightarrow \pi^*$ transition from the meso nitrogen of the macrocycle [9, 13].

3.1.3 2,3,9,10,16,17,23,24-octa substituted phthalocyanine **3a**

The ¹H NMR spectrum exhibited a signal with chemical shift -2.016 ppm characteristic of the pyrrolic protons in the core [13]. The signals at 7.6-6.8 ppm were assigned to the benzyl protons. On the other hand its infrared spectrum exhibited a band at 3620 cm⁻¹ assigned to the N-H stretching vibration [15]. The absence of the C≡N stretching band in the spectrum corroborated this further. It has been reported that the isoindole and pyrrole stretching frequencies serve as markers for phthalocyanine formation. This was observed at 1378-1465 cm⁻¹ and 1321 cm⁻¹ respectively [18-20]. Consequently they serve as further evidence for the formation of the macrocycle. Bands at 1091 cm⁻¹ and 1163 cm⁻¹ were assigned to pyrrole and isoindole (with some small contribution from C-H in-plane bending) breathing frequencies [18]. Aromatic C=C and *ortho*-substituted benzene stretch was observed at 1582 cm⁻¹ and 1685-1700 cm⁻¹ respectively [15]. The ultraviolet-visible spectrum gave characteristic B-band at $\lambda_{\text{max}} = 337$ nm. In the visible region two intense absorptions of comparable intensity were observed. These are due to the splitting of Q-band into Q_x [$\lambda_{\text{max}} = 666$ nm] and Q_y [$\lambda_{\text{max}} = 703$ nm]. This therefore confirmed the D_{2h} symmetry of **3a**. The transitions are assigned to $\pi \rightarrow \pi^*$ transitions [1, 21, 22].

3.1.4 Complexes

The characterizations of the complexes were carried out using elemental analysis, IR and Uv-vis spectrophotometric techniques and are presented in **Tables 1 and 2**. The spectral assignments for the complexes were achieved by comparing their vibrational frequencies with that of the free ligand. Absence of certain bands and shifts in others indicated coordination. Electronic spectra for some of the complexes and their ligands are given in **Figures 4 and 5**.

3.2 Kinetic studies of metalation

Preliminary repetitive scanning of the ultraviolet spectral region during the incorporation of Co(II) and Cu(II) in **1a**, **2a** and **3a** gave well defined isobestic points (**Table 3**) for over two half-lives for the individual reactions. Typical spectra changes for these reactions are presented in **Figure 6**. The plots of $1/[A]$ versus time were linear, suggesting second order kinetics (**Figure 7**).

A comparative analysis showed that the rate of incorporation of the metal ions into the central cavity of the ligands is a function of the metal ion and peripheral functionalities of the ligands. Generally the cobalt(II) complexes were more readily formed than the corresponding copper(II) complexes. This fact is more evident in the coordination of **2a** and **3a**, for which there was significant difference in the metalation rate for both metal ions. An explanation based on difference in size could be used here [23], since cobalt(II) ion is larger than Cu(II) ion. According to Hambright and Chock [24], these macrocycles deform causing their nucleus to rearrange to provide a suitable configuration for metalation. It is therefore suggested that as a result of the bigger size of Co(II) ion there is less strain on the pyrrolic nitrogen of the macrocycles on coordination. On the other hand the nucleus would have to bend, stretching itself on coordination to Cu(II) ion as a result of its size. This creates strain on the nucleus. There is however, no significant difference in metalation rate for both **1b** and **1c**. It is proposed that the highly symmetrical nature and flexibility of the peripheral functionality induces a form of flexibility on the cavity of the ligand. Although the rate of incorporation of Co(II) ion was still slightly higher (**Table 4**). Further lending credit to the size argument.

The rate of metalation, between the ligands was of the order **2a** > **1a** > **3a** for both metal ions. The difference in the reactivity can be interpreted by considering the electronic and steric effect of the peripheral functionalities of the ligands. The macrocycle with the greater basicity reacts with the metal ions faster. Such similar correlation was observed by Worthinton et al. and Inamo et al. for porphyrins [25, 26]. This is because the outer sphere association between the deformed macrocycles and the metal(II) ions prior to coordination is considered to be driven by an electrostatic attraction between the local negative charge on the pyrrolic nitrogen and the positive charge on the metal ion [26, 27]. Further difference in the rates of complexation of the ligands is attributable to the steric hindrance brought about by the relative rigidity of the various peripheral substituents of the ligands [28]. This is reflected in **2a** with unsymmetrical peripheral functionalities giving a deformed central cavity. Although the rigid benzo group induces some rigidity on the porphyrine ring the dimethylamino substituent is more flexible [29]. This flexibility creates a form of allowance for the deformation of the ring. Consequently it compels the porphyrine ring system to be more favourably distorted for complexation. This is in agreement with that reported for porphyrins with unsymmetrical central nucleus [23]. It is suggested in the case of **1a** that as a result of its more flexible

functionalization, its core is deformed to a great extent for it to effectively coordinate with the metal ions in the course of complex formation [26]. This and the symmetrical nature of the peripheral functionality, support the fact that the rate of insertion is similar for both metal ions. In the **3a** complex, the peripheral functionalities induce a form of rigidity on the macrocycle inhibiting its deformation. Consequently the central cavity is more defined. The electrostatic approach between the metal ion and the deformed **1a** ring is thus restricted by this steric effect [26]. Hence slow rate of insertion. This is supported by the fact that at higher temperature the rate for insertion for the Co(II) ion increased. It is suggested that increasing the temperature enabled the ligand to rearrange itself, attain a form of better flexibility enabling it to deform in such a way for easy complexation of the metal ions [29]. This is corroborated by Hambright and Chock [24], who proposed that slow rates for similar macrocycles are accounted for in part to the unfavourable deformation equilibria [24]. This is further supported by the high activation entropy for the reaction (**Table4**).

3.3 Mechanism of metal ion incorporation.

All the reactions studied in this research were over 95% complete and the observed rate constants were obtained from plots of $1/[A]_t$ against time, which gave a straight line where A_t = absorbance at time t. The following scheme represents the possible pathways for the incorporation of the metal ions into the central cavity of **1a**

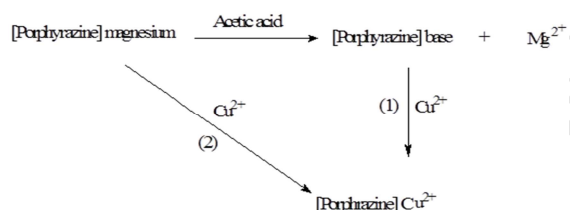


Figure 8. Proposed reaction pathway for the metalation of **1a**

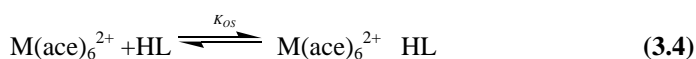
Pathway (1) is proposed to be the removal of the central magnesium(II) metal ion from the macrocycle, followed by a fast pick up of the metal(II) ion by the resulting free base (**Figure 8**). Pathway (2) involves the direct exchange of positions between the Cu(II) metal ion and magnesium in **1d** without forming the free base first (**Figure 8**). This reaction pathway involves the formation of the heterodinuclear metaloporphyrine complex intermediate. Thus it has two different metal ions bound simultaneously to the ligand on the opposite sides [23, 30].

Process for reaction system being



According to the activation energy requirements however, pathway (1) is the more plausible mechanism. The activation energy requirement for the metalation of **1a** is lower in pathway (1) (Table 4.). Indicating that magnesium has to be removed first before the incorporation of another metal ion

From section 3.2 above the deformation of the macrocycle is required for the metal ion to effectively interact with the nitrogen atom of the pyrrole group. It is proposed that in line with most mechanisms the macrocycles form an outer sphere complex with the metal species [24]. From previous studies the rate determining step for the metalation of these macrocycles is the dissociation of a coordinated solvent molecule from the metal ion in the outer-sphere associated complex [23, 24]. Based on these, the rate law for the reactions may be giving by the product of equilibrium constant for the deformation of the rings K_D , equilibrium constant for the outer sphere complex formation K_{OS} and the rate constant for the dissociation of the coordinating solvent molecules in the inner sphere of the metal(II) ion k_i .



Where:

L= **1a**, **2a**, and **3a**

M= Co(II) and Cu(II)

K_D = equilibrium constant for the deformation of the rings

K_{OS} = equilibrium constant for the outer sphere complex formation

k_i = rate constant for the dissociation of the coordinating solvent molecules in the inner sphere of the metal(II) ion

3.4 Kinetics of redox reaction

During the redox reaction involving Cu(II)L (L= **1a**, **2a** and **3a**) and cobalt(II) complex of **1a**, preliminary repetitive scanning of the ultraviolet-visible spectral region gave well defined isobestic points for more than two half-lives for the individual reactions (Table 3) and (Figures 9-11). This signifies that a single reduced species was formed during the reactions [1, 4, 8]. The plots of $1/[A]$ versus time were linear, which suggested that the reactions followed second order kinetics.

Tetrapyrrole macrocyclic complexes are capable of successive four ring reduction and two ring oxidation steps. Consequently they may act as oxidizing and or reducing agents [7, 8]. From previous reports their redox activity may be metal or ligand based [1, 2, 4, 8]. This activity is dependent on the availability of low energy orbital for charge transfer [2]. In this study a spectrophotometric method was used to study the kinetics of redox reaction of **1c**, **2c** and **3c** with **1b**. The spectral changes observed during the redox reaction of **1c** and **1b** (**Figure 9**) showed the Q-band increased in intensity with a hypsochromic shift from 581 to 627 nm and a new band was observed at 509 nm. Previous studies have reported that these are characteristic features for the formation of the π -anion radical for tetrapyrrole macrocyclic complexes with redox inactive central metals [1, 2, 8, 31]. Further evidence for the ring reduction was given by the weak broad band attributable to the $d-d$ transition; $B_{1g} \rightarrow E_g$ indicative of Jahn Teller distorted Cu^{2+} which shifted hypsochromically from 665 to 700 nm with increase in intensity [32]. The redox process resulted in clear isobestic points obtained at 581 and 822 nm in the spectrum. On the other hand the spectroscopic changes recorded during the redox reaction involving **2c** and **1b** (**Figure 10**) showed a shift in the Q-band from 556 to 590 nm with decrease in intensity. Two new bands were recorded at 560 and 627 nm. Similar spectroscopic changes have been reported by Tuncer et al. [1] as characteristic of porphyrazine ring reduction. The broad band ascribable to a tetragonally distorted Cu^{2+} $B_{1g} \rightarrow E_g$ transition [32] further suggests a ligand based reduction. The redox process however resulted in clear isobestic points at 580 and 620 nm. **Figure 11** represents the spectral changes which occurred during the reduction of **3c**. The Q band red shifted from 667 to 590 nm with retention of intensity. Two new bands were observed at 558 and 628 nm. According to Donzello et al. [31] these are suggestive of the formation of a π -anion radical of a tetrapyrrole macrocycle. The broad band characteristic of a tetragonal distorted Cu^{2+} $B_{1g} \rightarrow E_g$ shifted from 700 to 673 nm. Clear isobestic points were observed at 577 and 620 nm in the spectrum [32]. It is therefore proposed that the Co(II) ion reduced the Cu(II) complexes to give a π -anion with the Co(II) ion oxidized to Co(III). This is supported by previous studies that showed that first oxidation takes place on the metal ion for Co(II) complexes of these macrocycles. According to these studies donor solvents strongly favour trivalent cobalt formation by coordinating in axial positions to form six-coordinate $L_2Co(III)L$ species. In the absence of donors molecules oxidation to Co(III) is inhibited and ring oxidation occurs first [2, 7, 8, 33]. This is suggestive of the availability of a low energy d -orbital electron for charge transfer in the octahedral geometry of Co(II) as opposed to the square planar geometry. According to Lever et al. [2] this electron lies between the HOMO (π) and LUMO (π^*) orbitals of the ligands [2, 8]. The broad bands ascribed to Jahn Teller distorted Cu(II) ion, further confirmed the fact that reduction for the Cu(II) complexes was ligand based and not metal based.

The trend for the rate of the reduction followed the order $2c > 1c > 3c$ (Table 4). It is suggested that the reduction rate is influenced by the ring substituents. This is reflected more in the $2c$ complex with electron rich substituents. The ease of reduction of this compound as compared to the other complexes may be attributed to the formation an unstable species necessitating the subsequent diffusion of charge. As a consequence it is suggested that the ring reduction is succeeded by another reaction, possibly the diffusion of charge [7, 8, 34].

Generally the rate of reaction was relatively slow compared to similar reactions [35]. Although such reactions are fast, for acyclic compounds, the size of the macrocycle affected the rate. For the reaction to take place the reactants have to rearrange before electron transfer could take place to satisfy the Franck Condon requirements. This stipulates that the oxidant and the reductant must reorganised themselves before the act of electron transfer in a way that ensures that the energies of the oxidant and reductant in their transition state are identical. Tetrapyrrole macrocycles are relatively large and as such take time to rearrange. This inevitably slows the reaction. Therefore it can be implied that the rate of the reaction is also dependent on the rate of rearrangement of the macrocycles (Table 4). From the foregoing therefore, an outer sphere mechanism is proposed for the reactions. This is because the coordination sphere of both reductants and oxidants remain the same after the reactions. There is also no bridging group common to the coordination sphere of both; consequently the reactions followed an electron tunnelling mechanism.

4.0 Conclusion

The study has shown the significance of peripheral substituents and metal size in tuning the reactivity of tetrapyrrole macrocyclic compounds. It also underscores the effect of the deformation of the central cavity for effective metalation. It also highlighted the need to obtain the free base before the incorporation of desired metal ion into the central cavity of these macrocycles. The study further showed that the rate of redox reaction of the complexes is a function of their peripheral functionalities.

Acknowledgements

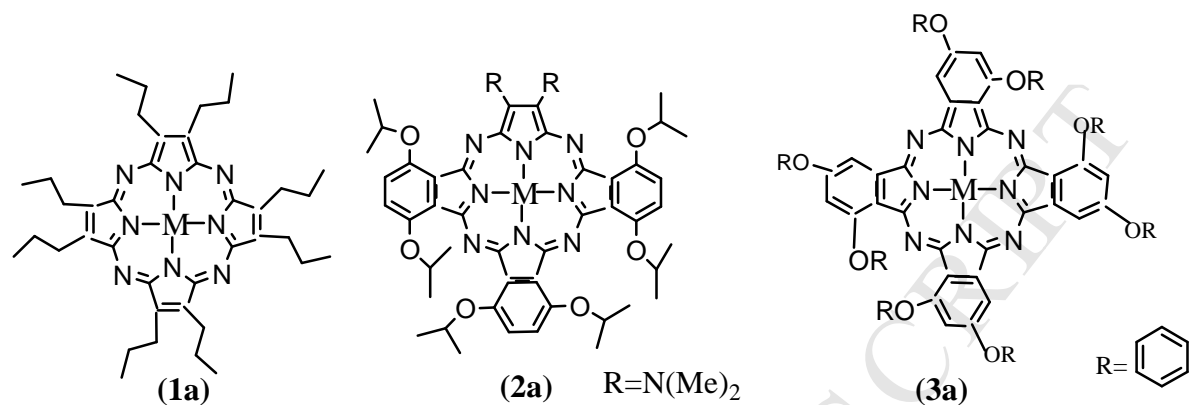
The authors thank Prof BDG Williams, formerly of the University of Johannesburg, for the use of his laboratory, meaningful suggestions and discussions and the North-West University Material Science Innovation and Modelling (MaSIM) research focus area for funding.

References

- [1] Tuncer S, Koca A, Gül A, Avcıata U. Synthesis, characterization, electrochemistry and spectroelectrochemistry of novel soluble porphyrazines bearing unsaturated functional groups. *Dyes Pigments* 2012; 92:610-618.
- [2] Lever A, Pickens S, Minor P *et al.* Charge-transfer spectra of metallophthalocyanines: correlation with electrode potentials. *J Am Chem Soc* 1981; 103:6800-6806.
- [3] Schramm CJ, Hoffman BM. Octakis (alkylthio) tetraazaporphyrins. *Inorg Chem* 1980; 19:383-385.
- [4] Tuncer S, Koca A, Gül A, Avcıata U. 1, 4-Dithiaheterocycle-fused porphyrazines: Synthesis, characterization, voltammetric and spectroelectrochemical properties. *Dyes Pigments* 2009; 81:144-151.
- [5] Karadeniz H, Gök Y, Kantekin H. The synthesis and characterization of new metal-free and metalloporphyrazine containing macrobicyclic moieties. *Dyes and pigments* 2007; 75:498-504.
- [6] Michel S, Hoffman B, Baum S, Barrett A. *Progress in inorganic chemistry*. John Wiley and Sons, New York 2001; 5:473-590.
- [7] Yıldız G, Akkuş H, Gül A. A Cyclic Voltammetric Study of Some Porphyrazines. *Monatsh Chem /Chem Mon* 2001; 132:659-667.
- [8] Koca A, Sağlam ÖG, Gül A. Electrochemical investigation on porphyrazines with peripheral crown-ether groups. *Monatsh Chem/Chem Mon* 2003; 134:11-21.
- [9] Forsyth TP, Williams DBG, Montalban AG *et al.* A facile and regioselective synthesis of trans-heterofunctionalized porphyrazine derivatives. *J Org Chem* 1998; 63:331-336.
- [10] Sesalan ŞB, Gül A. Synthesis and Characterization of a Phthalocyanine-Porphyrazine Hybrid and its Palladium (II) Complex. *Monatsh Chem/Chem Mon* 2000; 131:1191-1195.
- [11] Kandaz M, Michel SL, Hoffman BM. Functional solitare-and trans-hybrids, the synthesis, characterization, electrochemistry and reactivity of porphyrazine/phthalocyanine hybrids bearing nitro and amino functionality. *J Porphyr Phthalocyanines* 2003; 7:700-712.
- [12] Fitzgerald JP, Haggerty BS, Rheingold AL *et al.* Iron octaethyltetraazaporphyrins: synthesis, characterization, coordination chemistry, and comparisons to related iron porphyrins and phthalocyanines. *Inorganic Chemistry* 1992; 31:2006-2013.
- [13] Gonca E, Köseoğlu Y, Aktaş B, Gül A. Octakis (1-naphthylmethylthio) substituted porphyrazine derivatives. *Polyhedron* 2004; 23:1845-1849.
- [14] Stuzhin P, Pimkov I, Ul A *et al.* Synthesis and spectral properties of 1, 2, 5-thiadiazolo-, 1, 2, 5-selenadiazolo-, and benzo-fused β -phenyl-substituted porphyrazines. *Russ J Org Chem* 2007; 43:1854-1863.

- [15] Kemp W. Organic spectroscopy. Edinburgh 1991.
- [16] Nakamoto K. Infrared spectra of inorganic and coordination compounds. 1970.
- [17] Stuzhin P. Investigation of unsubstituted porphyrine by proton NMR and the structure of porphyrine ligands. *Chem Heterocycl Comp* 1997; 33:1185-1190.
- [18] Lu F, Bao M, Ma C *et al.* Infrared spectra of phthalocyanine and naphthalocyanine in sandwich-type (na) phthalocyaninato and porphyrinato rare earth complexes. Part 3. The effects of substituents and molecular symmetry on the infrared characteristics of phthalocyanine in bis (phthalocyaninato) rare earth complexes. *Spectrochim Acta Part A: Mol Biomol Spectros* 2003; 59:3273-3286.
- [19] Bao M, Bian Y, Rintoul L *et al.* Vibrational spectroscopy of phthalocyanine and naphthalocyanine in sandwich-type (na) phthalocyaninato and porphyrinato rare earth complexes:(part 10) the infrared and Raman characteristics of phthalocyanine in heteroleptic bis (phthalocyaninato) rare earth complexes with decreased molecular symmetry. *Vib Spectrosc* 2004; 34:283-291.
- [20] Montalban AG, Michel SL, Baum SM *et al.* Lanthanide porphyrine sandwich complexes: synthetic, structural and spectroscopic investigations. *J Chem Soc, Dalton Trans* 2001; 22:3269-3273.
- [21] Stuzhin P, Bauer E, Ercolani C. Tetrakis (thiadiazole) porphyrines. 1. Syntheses and properties of tetrakis (thiadiazole) porphyrine and its magnesium and copper derivatives. *Inorg Chem* 1998; 37:1533-1539.
- [22] Shimizu S, Ito Y, Oniwa K *et al.* Synthesis of 5, 10, 15-triazaporphyrins—effect of benzo-annulation on the electronic structures. *Chem Comm* 2012; 48:3851-3853.
- [23] Funahashi S, Inada Y, Inamo M. Dynamic study of metal-ion incorporation into porphyrins based on the dynamic characterization of metal ions and on sitting-atop complex formation. *Anal Sci* 2001; 17:917-928.
- [24] Hambright P, Chock P. Metal-porphyrin interactions. III. Dissociative-interchange mechanism for metal ion incorporation into porphyrin molecules. *J Am Chem Soc* 1974; 96:3123-3131.
- [25] Worthington P, Hambright P, Williams R *et al.* Reduction potentials of seventy-five free base porphyrin molecules: Reactivity correlations and the prediction of potentials. *J Inorg Biochem* 1980; 12:281-291.
- [26] Inamo M, Kamiya N, Inada Y *et al.* Structural characterization and formation kinetics of sitting-atop (SAT) complexes of some porphyrins with copper (II) ion in aqueous acetonitrile relevant to porphyrin metalation mechanism. Structures of aquacopper (II) and Cu (II)-SAT complexes as determined by XAFS spectroscopy. *Inorg Chem* 2001; 40:5636-5644.
- [27] Turay J, Hambright P. Activation parameters and a mechanism for metal-porphyrin formation reactions. *Inorg Chem* 1980; 19:562-564.

- [28] Bain-Ackerman MJ, Lavalley DK. Kinetics of metal-ion complexation with n-methyltetraphenylporphyrin. Evidence concerning a general mechanism of porphyrin metalation. *Inorg Chem* 1979; 18:3358-3364.
- [29] Inada Y, Sugimoto Y, Nakano Y *et al.* Formation and deprotonation kinetics of the sitting-atop complex of copper (II) ion with 5, 10, 15, 20-tetraphenylporphyrin relevant to the porphyrin metalation mechanism. Structure of copper (II)-pyridine complexes in acetonitrile as determined by exafs spectroscopy. *Inorg Chem* 1998; 37:5519-5526.
- [30] Tabata M, Miyata W, Nahar N. Kinetics and mechanism of metal-substitution reaction of homodinuclear mercury (II) porphyrin with zinc (II) with particular reference to a heterodinuclear metalloporphyrin intermediate. *Inorg Chem* 1995; 34:6492-6496.
- [31] Donzello MP, Agostinetto R, Ivanova SS *et al.* Tetrakis (thiadiazole) porphyrazines. 4. direct template synthesis, structure, general physicochemical behavior, and redox properties of AlIII, GaIII, and InIII complexes. *Inorg Chem* 2005; 44:8539-8551.
- [32] Greenwood NN, Earnshaw A, Earnshaw A. *Chemistry of the Elements*. Pergamon press Oxford etc.; 1984.
- [33] Erdoğan A, Koca A, Avciata U, Gül A. Synthesis, Characterization and Electrochemistry of New Soluble Porphyrazine Complexes Bearing Octakis 3-Methylbutylthio Substituents. *Z Anorg Allg Chem* 2008; 634:2649-2654.
- [34] Ikeuchi H, Kanakubo M. Determination of diffusion coefficients of the electrode reaction products by the double potential step chronoamperometry at small disk electrodes. *J Electroanal Chem* 2000; 493:93-99.
- [35] Tobe M-L. *Inorganic Reaction Mechanisms* (Nelson, London, 1972). Search PubMed 1974.



1a, 2a, 3a; M=Zn

1b, 2b, 3b; M=Co(II)

1c, 2c, 3c; M=Cu(II)

1d; M=Mg(II)

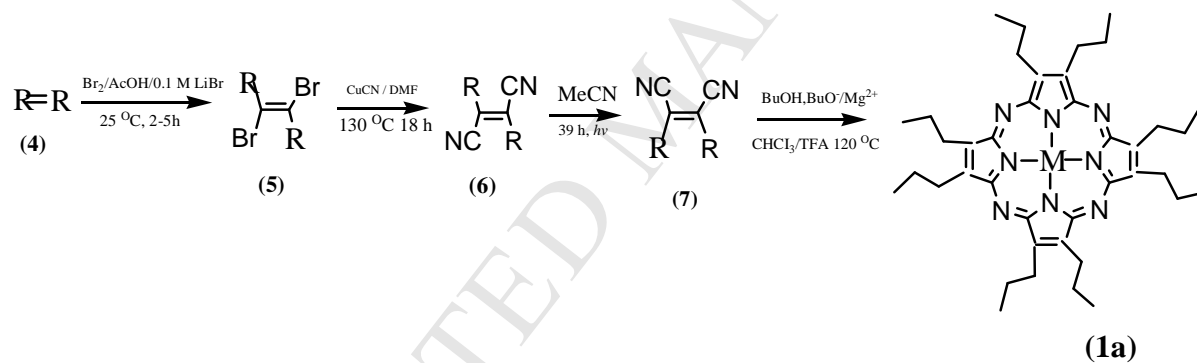


Figure 1. Reaction scheme for the formation of **1a**

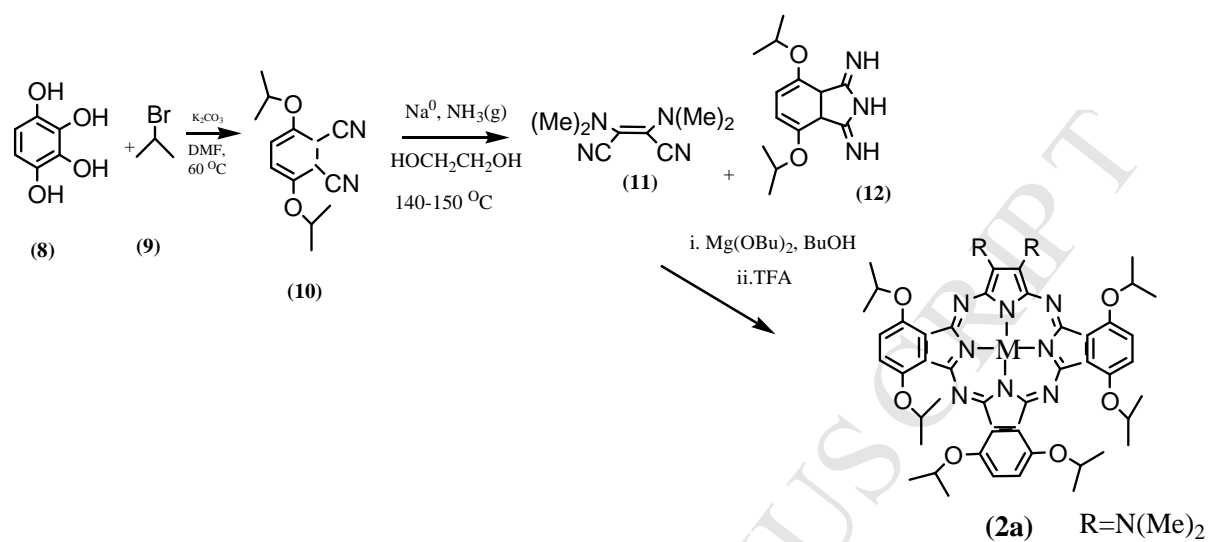


Figure 2. Reaction scheme for the formation of **2a**

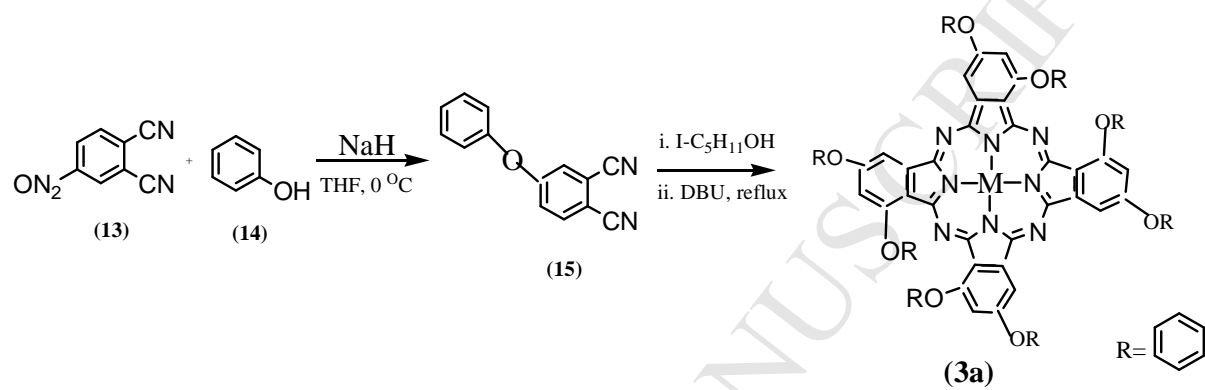


Figure 3. Reaction scheme for the formation of 3a

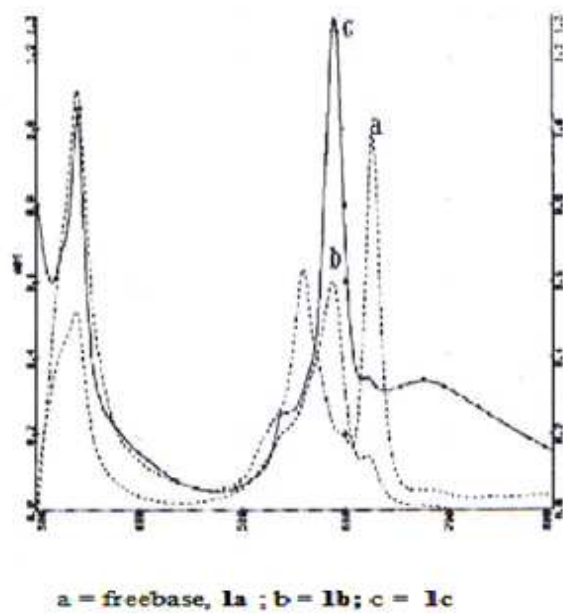


Figure 4. Uv-vis spectra for **1a**, **1b** and **1c**

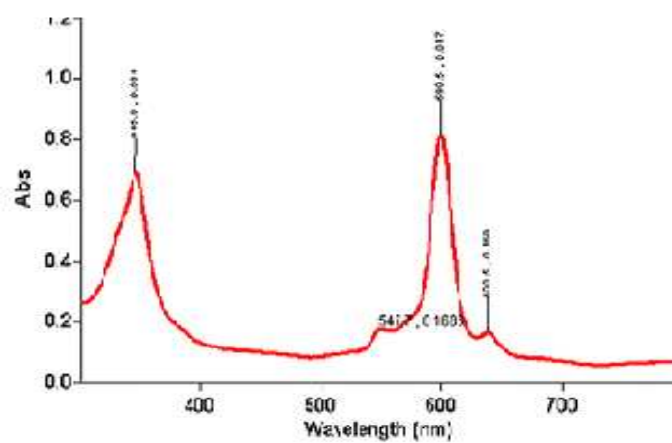


Figure 5. Uv-vis spectrum of **1d**

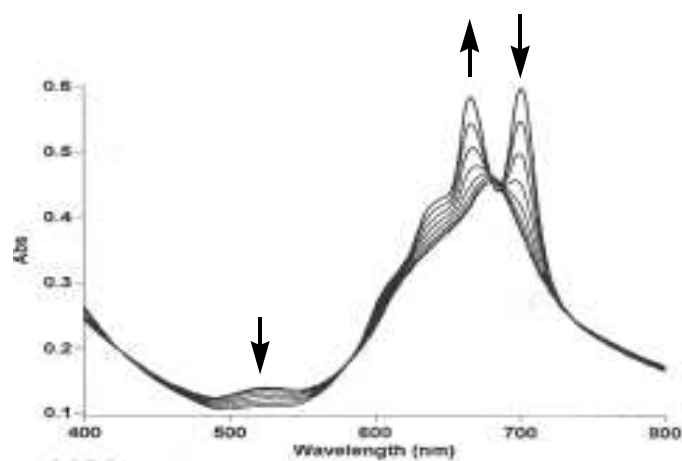


Figure 6. Spectral changes during the reaction

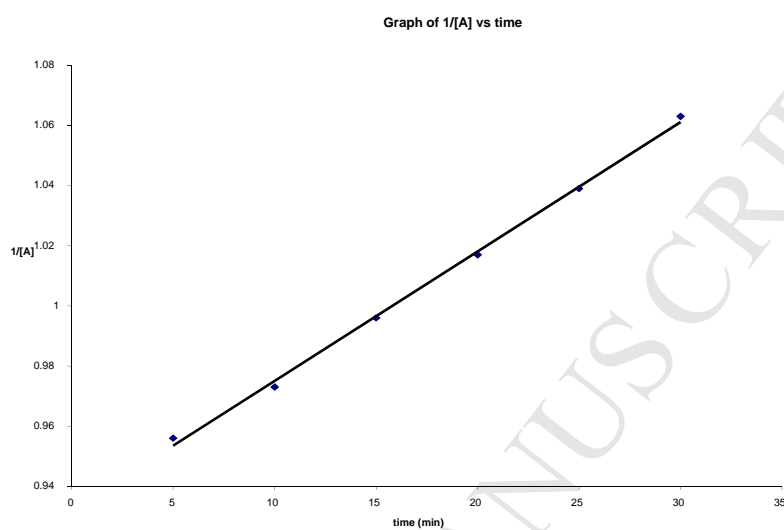


Figure 7. A typical kinetic plot for the metalation of **1a** free base with copper(II) ion at 25 °C

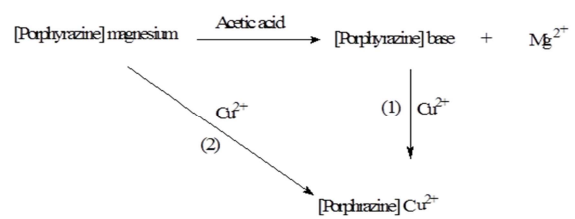


Figure 8. Proposed reaction pathway for the metalation of **1a**

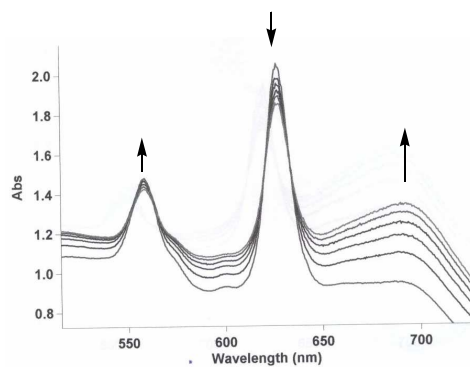


Figure 9. Spectral changes during the reduction of **1c** by **1b** at 25 °C

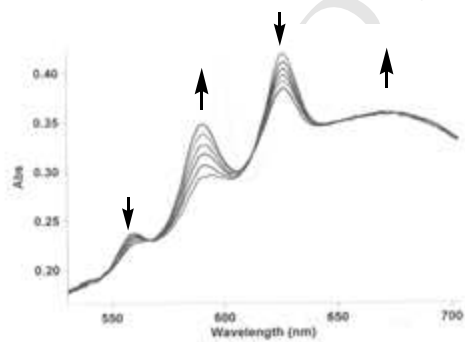


Figure 10. Spectral changes during the reduction of **2c** by **1b** at 25 °C.

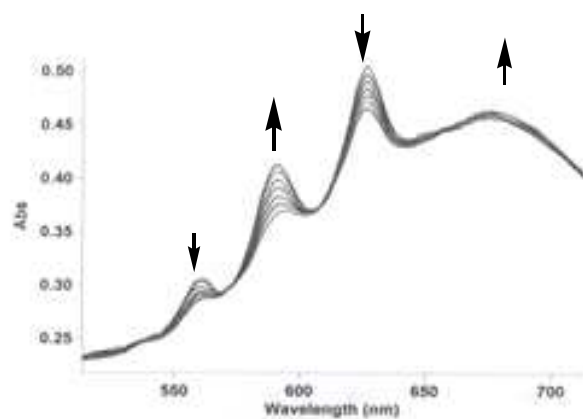


Figure 11. Spectral changes during the reduction of **3c** by **1b** at 25 °C at λ - 588 nm

Table 1. Infra-red stretching frequencies of the ligands and their complexes (cm⁻¹)

Compound	(N-H)	(CH ₂ , CH ₃)	(C-H)	(C=C)	(C-H)	(C-O)	(C-C)
1a	3021	2928-2851	1464	1209			
2a	3508			1593			
3a	3620			1685	2848		
1b		2824-2897		1644	3051		
1c		2925-2854		1640	3055		
2b					2997	1112	
2c				1660	3001		1013
3b		2770-2897		1586	2999		
3c		2856-2746		1579	2986		

Table2. UV-Vis spectra bands (nm) and elemental analysis of the ligands and their complexes

Compound	B	Q_x	Q_y	<i>d-d</i>	C, H, N (CALCULATED)
1a	339	558	626		71.68 (71.74); 8.01 (7.97); 20.28 (20.29)
2a	325	556	742		65.63 (64.49); 7.88 (7.29); 6.73 (6.47)
3a	337	661	703		76.21 (76.45); 4.18 (4.19); 9.11 (9.03)
1b	340	589		629	65.00 (65.03); 6.86 (6.90); 18.32 (18.39)
1c	336	581		665	64.50 (64.54); 6.81 (6.85); 18.00 (18.25)
2b	322	557		743	61.27 (60, 74); 6.33 (6.59); 15.02 (15.39)
2c	320	556		745	61.11 (60.40); 6.54 (6.56); 14.98 (15.32)
3b	330	669		700	72.88 (72.98); 3.80 (3.84); 8.48 (8.62)
3c	332	667		699	72.68 (72.72); 3.86 (3.83); 8.45 (8.59)

Table3. Isobestic points for kinetic reactions (nm)

Compound	Isobestic points^a	Isobestic points^b
1c	605, 566	581, 622
2c	720	580, 620
3c	690	577, 620
1b	560, 620	
2b	780, 820, 840	
3b	590, 715	
1d	540, 580, 624	

^a= Isobestic points obtained from the spectra for metalation

^b= Isobestic points obtained from the spectra for redox reactions

Table4. Rate constant, K (25.0 °C) and activation entropy, ΔS^\ddagger for the kinetic reactions

Compound	K^c ($M^{-1}s^{-1}$)	$\Delta S^{\ddagger c}$ ($JK^{-1}mol^{-1}$)	K^d ($M^{-1}s^{-1}$)	$\Delta S^{\ddagger d}$ ($JK^{-1}mol^{-1}$)
1c	2.70	78.56	10.0	188
2c	2.90	344.0	22.0	305
3c	0.51	241.7	12.30	22
1b	2.81	186.65		
2b	45.21	374.9		
3b	1.97	736.4v		
1d	0.50	1131.95		

^c=metalation^d= redox reaction